Adam Piłat*, Piotr Włodarczyk**

The μ-Synthesis and Analysis of the Robust Controller for the Active Magnetic Levitation System

1. Introduction

Over the centuries object suspension has stunned and interested most of the people including famous scientists such as Benjamin Franklin and Robert Goddard. In 1842 Ernshaw came up with the idea of the suspension of an object in the magnetic field created by permanent magnets. He also proved that permanent magnets cannot reach a stable levitation in all 6DOF [5] which requires new methods to be applied. The stable levitation is achieved by adjusting an object position and/or velocity feedback which creates the appropriate magnetic field. Active Magnetic Levitation System (AMLS) is a perfect example of a structurally unstable object. The control task is to maintain a ferromagnetic object in a desired position by generating an appropriate magnetic field which disposes of gravity and counteracts other accelerations.

In various magnetic levitation applications e.g. in high-speed trains and magnetic bearings [13,4] we face a problem of keeping the system stable even in the presence of parameters variations and other perturbations. Very common problem can be the control task of magnetic vehicles when the mass of passengers is variable. The synthesis and analysis of the robust controller for the AMLS with variable load one can find in [12,15].

Systems that can tolerate plant variability and uncertainty are called robust. The problem of stabilising the uncertain linear dynamic systems has been discussed and analysed for almost 3 decades. The main issue with control systems are differences between the actual system and its nominal model which is used in control system design. Every practising control engineer should take into account a real-world systems vulnerability to various types of perturbations like non-ideal sensors, actuators, external noises, parametric uncertainties, unmodelled non-linearities and many others. Methods based on modern feedback $\mathscr{H}_\infty$ optimisation theory [7,9,18] deal with robustness much more directly than other approaches.

* AGH University of Science and Technology, Faculty of Electrical Engineering, Autamatics, Computer Science and Electronics, Department of Automatics, Al. Mickiewicza 30, 30-059 Krakow, Poland. E-mail: ap@agh.edu.pl

** Ph.D. student at AGH University of Science and Technology, Faculty of Electrical Engineering, Automatics, Computer Science and Electronics, Department of Automatics, Al. Mickiewicza 30, 30-059 Krakow, Poland. E-mail: pwlodar@agh.edu.pl

The research on robust controllers design is said to be started in the late 1970s and early 1980s with a breakthrough paper by Zames [16] which introduced theory which was quickly extended to more general problems. At the time, active research on adaptation of this robust control theory to non-linear systems is being done in e.g. [1].

2. Active Magnetic Levitation System

2.1. Experimental Set Up

In the following research the INTECO active magnetic levitation system [8] was used. It is equipped with a coil current driver, an optical distance sensor and a computer-based real-time system. The schematic diagram with state variables and main forces as well as its photography is depicted in Figure 1. As it has been already mentioned the electromagnet located on the top of the device generates the magnetic field to keep a ferromagnetic object in a desired position.

Three typical ways of controlling the current in the electromagnet coil are used in AMLS: based on analogue voltage control, PWM signal control and current control [11]. Each of them has different features and influences the system dynamics in other way. In this case PWM voltage driven coil was applied and appropriate coefficients were included in the model equations.

Four objects were chosen to be tested in the experiments. They are divided into two groups of different diameter. In each group the objects have various mass. They weigh 0.05297 kg and 0.03140 kg in the first set and 0.05843 kg and 0.03693 kg in the second one, respectively. The objective of such a choice was to check the impact of the object size and mass on the controller behaviour.

a) b)

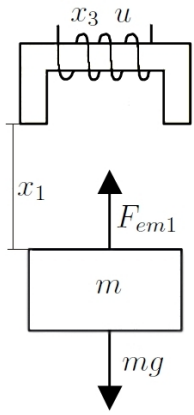

Fig. 1. Photo of the laboratory AMLS (a). Diagram of the AMLS with one electromagnet (b) [8]

2.2. System Dynamics

2.2.1. Non-linear Model

AMLS model proposed in [8] was applied with small modifications, as in the given AMLS only upper electromagnet is provided. Non-linear state-space equations describing the AMLS corresponding to the diagram from Figure 1 are given as follows:

$$\begin{cases} \dot{x_1} = x_2 \\ \dot{x_2} = -\dfrac{F_{em1}}{m} + g \\ \dot{x_3} = \dfrac{1}{f_i(x_1)}\Big(k_i u + c_i - x_3\Big), \end{cases} \tag{1}$$

where

$$f_i(x_1) = \frac{f_{iP1}}{f_{iP2}} exp\Big(\frac{-x_1}{f_{iP2}}\Big) \tag{2}$$

$$F_{em1}(x_1) = x_1^3 \frac{F_{emP1}}{F_{emP2}} exp\Big(\frac{-x_1}{F_{emP2}}\Big). \tag{3}$$

x_1 is a ferromagnetic object distance from an electromagnet, x_2 is an object velocity and x_3 is a current in a coil. F_{em1} is an electromagnetic force generated by the electromagnet. Both $F_{em1}, f_i(x_1)$ depend on the object distance from the electromagnet and the former also on the current in a coil. Those functions were chosen experimentally and seem to be appropriate ones. All model coefficients and parameters values and descriptions are given in Table 1.

Table 1
Model Parameters Values

Parameter	Description	Value	Unit
m	object mass	0.025-0.086	[kg]
g	gravitational acceleration	9.81	[m/s^2]
F_{em1}	Electromagnetic force	function of x1 and x3	[N]
F_{emP1}	Coefficient	6.5800e-003	[H]
F_{emP2}	Coefficient 2	6.1382e-003	[m]
$f_i(x_1)$		function of x1	[1/s]
f_{iP1}	Coefficient 3	744.3638e-006	[m·s]
f_{iP2}	Coefficient 4	6.6351e-003	[m]
c_i	Coefficient 5	-53.3046e-003	[A]
ki	Coefficient 6	3.8149	[A]
i_{MIN}	Minimal Current	0.03884	[A]
u_{MIN}	Minimal Voltage	0.00498	[V]

2.2.2. Linear Model

For the application of $\mathscr{H}_\infty$ optimisation method, the non-linear model (1) was linearised in an equilibrium point $x_0 = [x_{10} \quad x_{20} \quad x_{30}]^T$:

$$\begin{cases} \dot{x} = Ax + Bu \\ y = Cx \end{cases},$$

with matrices:

$$A = \begin{bmatrix} 0 & 1 & 0 \\ a_{21} & 0 & a_{23} \\ a_{31} & 0 & a_{33} \end{bmatrix}, \quad B = \begin{bmatrix} 0 \\ 0 \\ b_3 \end{bmatrix} \tag{4}$$

$$C = \begin{bmatrix} 1 & 0 & 0 \end{bmatrix}.$$

The coefficients in matrices A and B have the following form:

$$\begin{aligned} a_{21} &= \frac{x_{30}^2}{m} \frac{F_{emP1}}{F_{emP2}^2} exp(-x_{10}/F_{emP1}) \\ a_{23} &= -\frac{2x_{30}}{m} \frac{F_{emP1}}{F_{emP2}^2} exp(-x_{10}/F_{emP1}) \\ a_{31} &= \frac{c_i - x_{30}}{f_i(x_{10}) \cdot f_{iP2}} \\ a_{33} &= -f_i(x_{10})^{-1} \\ b_3 &= \frac{k_i}{f_i(x_{10})}. \end{aligned} \tag{5}$$

The steady-state point was chosen as follows. The desired position of a ferromagnetic object is $x_{10} = 0.01$. The object velocity must be equal to zero, thus $x_{20} = 0$. From the second equation in (4) we obtain the value for $x_{30} = 1.4480$. The formula for x_{30} is presented below:

$$x_{30} = \sqrt{mg \frac{F_{emP2}}{F_{emP1}} exp\Big(\frac{x_{10}}{F_{emP1}}\Big)}. \tag{6}$$

Additionally, the plant is stabilised in the equilibrium point when a constant control signal $u_0 = 0.3935$ is adjusted. One can get its value from the third equation in (4). Again, the formula for u_0 is presented below:

$$u_0 = \frac{x_{30} - c_i}{k_i}. \tag{7}$$

AMLS was linearised in the equilibrium point $x_0 = [0.01 \quad 0 \quad 1.4480]^T$, thus, the following matrices were obtained:

$$A = \begin{bmatrix} 0 & 1 & 0 \\ 1598.1807 & 0 & -13.5496 \\ -9103.8413 & 0 & -40.2348 \end{bmatrix}, \; B = \begin{bmatrix} 0 \\ 0 \\ 1.5349 \end{bmatrix},$$

$$C = \begin{bmatrix} 1 & 0 & 0 \end{bmatrix}. \tag{8}$$

3. Robust Controller Design

3.1. Robust Modelling

In order to prepare a model for the robust analysis, parameter m was taken out of a_{21} and a_{23} coefficients. The experiments will be done for the objects whose mass varies. That is why it is convenient to represent the mass parameter in the following way:

$$m = \bar{m}(1 + p_m \delta_m), \tag{9}$$

where $\bar{m}$ is a nominal mass value, p_m denotes a percentage variance of the parameter and $\delta_m \in [-1, 1]$. To model uncertainty in a proper way the parameters were chosen as follows $p_m = 0.4$ and $\bar{m} = 0.04493$ after finding the mean of all masses. For the sake of the design we cite the Upper Linear Fractional Transformation (ULFT) definition [7]:

Definition 1 *(Upper Linear Fractional Transformation). Let M be a complex matrix partitioned as*

$$M = \begin{bmatrix} M_{11} & M_{12} \\ M_{21} & M_{22} \end{bmatrix} \in \mathbb{C}^{(p_1+p_2)\times(q_1+q_2)}, \tag{10}$$

and let $\Delta \in \mathbb{C}^{q_1 \times p_1}$ and $K \in \mathbb{C}^{q_2 \times p_2}$ be the other complex matrices. Then we can formally define an upper LFT with respect to Δ as the map:

$$\mathscr{F}_u(M, \cdot) : \mathbb{C}^{q_1 \times p_1} \to \mathbb{C}^{p_2 \times q_2} \tag{11}$$

with

$$\mathscr{F}_u(M, \Delta) = M_{22} + M_{21}\Delta(I - M_{11}\Delta)^{-1}M_{12} \tag{12}$$

provided that the inverse $(I - M_{11}K)^{-1}$ exists. ∎

Mass inverse will be presented in a form of ULFT with respect to M and δ_m:

$$\frac{1}{m} = \mathscr{F}_u(M, \delta_m) = \frac{1}{\bar{m}} - \frac{p_m}{\bar{m}}\delta_m(1 + p_m\delta_m)^{-1} \tag{13}$$

with

$$M = \begin{bmatrix} -p_m & \frac{1}{\bar{m}} \\ -p_m & \frac{1}{\bar{m}} \end{bmatrix}. \tag{14}$$

It introduces the following input/output relation to our system:

$$\begin{bmatrix} y_m \\ v_m \end{bmatrix} = \begin{bmatrix} -p_m & \frac{1}{\bar{m}} \\ -p_m & \frac{1}{\bar{m}} \end{bmatrix} \begin{bmatrix} u_m \\ a_{21}x_1 + a_{23}x_3 \end{bmatrix}. \tag{15}$$

which obviously modifies system equations to:

$$\begin{bmatrix} \dot{x_1} \\ \dot{x_2} \\ \dot{x_3} \\ y_m \\ y \end{bmatrix} = G_{ML} \begin{bmatrix} x_1 \\ x_2 \\ x_3 \\ u_m \\ u \end{bmatrix} \tag{16}$$

$$[u_m] = [y_m \delta_m],$$

where

$$G_{ML} = \begin{bmatrix} A & B_1 & B_2 \\ C_1 & D_{11} & D_{12} \\ C_2 & D_{21} & D_{22} \end{bmatrix}, \tag{17}$$

with matrices:

$$B_1 = \begin{bmatrix} 0 \\ -p_m \\ 0 \end{bmatrix}, \quad B_2 = \begin{bmatrix} 0 \\ 0 \\ b_3 \end{bmatrix}, \quad C_1 = \begin{bmatrix} a_{21} & 0 & a_{23} \end{bmatrix}, \quad C_2 = \begin{bmatrix} 1 & 0 & 0 \end{bmatrix},$$

$$D_{11} = -p_m, \quad D_{12} = D_{21} = D_{22} = 0.$$

G_{ML} denotes an input/output dynamics of the system (16) with parametric uncertainties. One can notice that it consists of the basic linear state-space equations (4) and the equations obtained by variations over m parameter (15). In Figure 2 Bode plots of the nominal and perturbed AMLS are depicted in order to present the impact of the mass variations on the plant to be compensated by a controller.

Furthermore, because in the given AMLS the position sensor is optical, shape and size affect the sensor characteristics which can be treated as a sensor noise to be cancelled by

weighting functions. Even though sensor characteristics are not very precise, differences must be taken into consideration when experiments results are discussed.

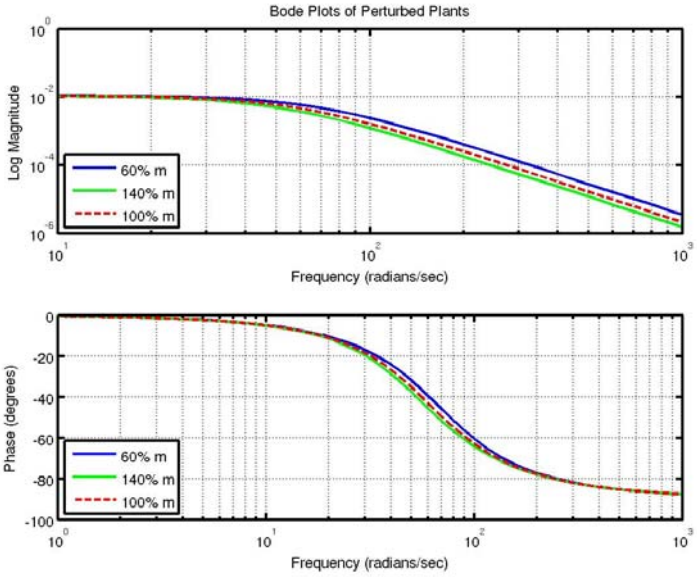

Fig. 2. Bode frequency responses of the nominal and perturbed plants

3.2. Design Requirements

Originally the problem of the $\mathscr{H}_\infty$ optimisation was proposed and solved by Zames in [16]. Let us define the sensitivity function of the continuous closed-loop system (Fig. 3):

$$S = (I + GK)^{-1}, \tag{18}$$

where G is the plant transfer function and K is the controller transfer function. The main objective of the $\mathscr{H}_\infty$ optimisation is to find a controller K that makes the closed-loop system stable and minimizes the peak value of the sensitivity function:

$$\min_K \|S\|_\infty = \min_K \sup_{\omega \in \mathbb{R}} \|S(j\omega)\|_2. \tag{19}$$

In general the $\mathscr{H}_\infty$ optimisation problem can be considered as the minimisation of the peak value of certain closed-loop frequency response functions [9,10]. In other words, $\mathscr{H}_\infty$ optimisation addresses the following two issues:

1) Closed-loop system with K must be asymptotically stable,
2) The influence of the disturbance d on the output y should be minimised.

3.2.1. Mixed Sensitivity Problem

To ensure the robust stability and performance specification by a robust controller the criteria that must be satisfied will be introduced briefly. The mixed sensitivity (or, so-called S over KS)[7] problem may be formulated as a special case of $\mathscr{H}_\infty$ optimal regulator problem [9]:

$$\min_{K stabilising} \left\| \begin{array}{c} W_p(I+GK)^{-1} \\ W_u K(I+GK)^{-1} \end{array} \right\|_\infty . \tag{20}$$

In fact, equation (20) describes the nominal performance criterion that must be satisfied by a control system depicted in Figure 3. It is the closed-loop system with model uncertainties and possible perturbations included. The system G in (20) as well as in Figure 3 refers to a transfer function combining G_{ML} (17) and uncertainties representation Δ (G is an ULFT ($\mathscr{F}_U(G_{ML},\Delta)$) with respect to G_{ML} and Δ).

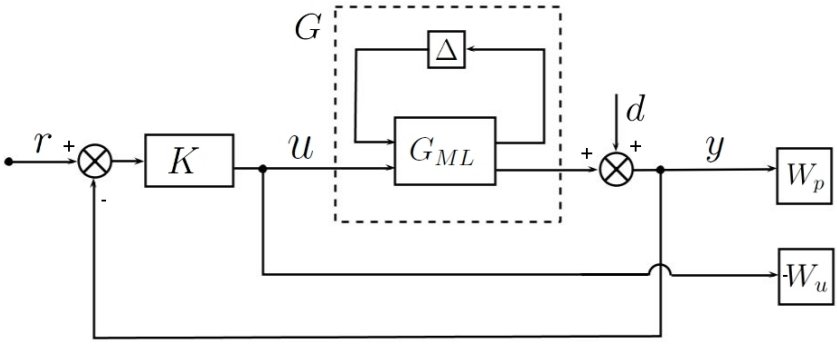

Fig. 3. Continuous closed-loop system structure

3.2.2. Weighting Functions Choice

The most crucial and difficult task in robust controller design is a choice of the weighting functions. In this case we have only two W_p and W_u which does not mean that the problem is less complex. Even though in some articles there are attempts to outline the algorithm for finding appropriate functions, it is still a very monotonous and laborious process especially when a given model has complex non-linearities which obviously are omitted in a linear model. The very general guidelines for weighting functions choice (21) were proposed in [3,17,14] and were used in this paper, though were not strictly followed:

$$W_p = \left(\frac{\frac{s}{M_p^{\frac{1}{n_p}}} + \omega_b}{s + \omega_b A_p^{\frac{1}{n_p}}} \right)^{n_p} \qquad W_u = \left(\frac{\tau s + A_u^{\frac{1}{n_u}}}{\frac{\tau s}{M_u^{\frac{1}{n_u}}} + 1} \right)^{n_u} , \tag{21}$$

where M_p and M_u are high frequency gains, A_p and A_u are low-frequency gains and ω_b and τ determine crossover frequency. n_p and n_u denote the order of a function. In literature there are also some articles about applying intelligent optimisation methods (genetic algorithms) [6,2] to find the best weighting functions however there is still a great deal of work to do in this field.

In the case of the given AMLS, W_p was chosen as a first-order scalar function presented below:

$$W_p = 100 \cdot \frac{0.1s + 2500}{14s + 3000}, \tag{22}$$

while W_u was taken as a constant value:

$$W_u = 10^{-2}. \tag{23}$$

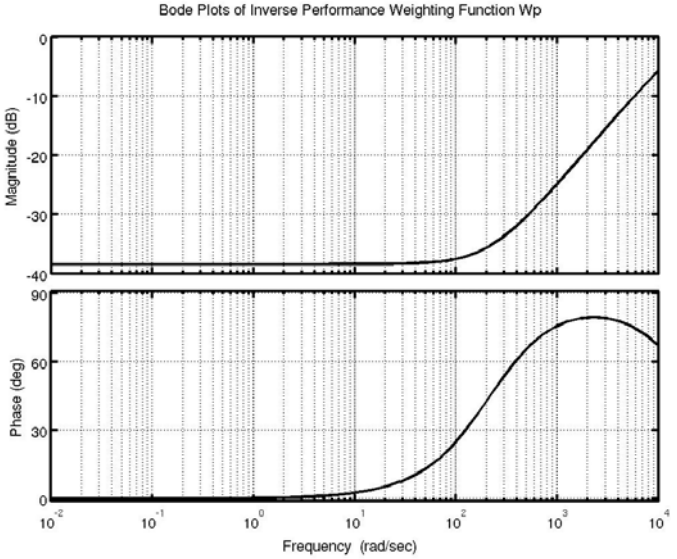

Fig. 4. Bode plots of inverted weighting function W_p

The entire procedure of choosing those weights was done experimentally with the help of the article [12] , however the objective of finding the controller of the lowest order and complexity determined the order of the designed functions (The less complicated functions are, the less compensator order is obtained). The aim of the weighting functions is to reflect the significance of meeting performance criteria within particular frequency range. Thus, performance weighting function was retrieved as (22). From (20) and the fact that W_p and W_u are scalar functions, it is seen that to ensure performance criteria, sensitivity function

singular values must lie below $\frac{1}{W_p}$. The singular values of the inverted weighting function W_p are presented in Figure 4.

Unfortunately, in real-world applications theory does not guarantee effectiveness of the obtained controller. Many trials were done to obtain a controller which stabilises a ferromagnetic object in a desired position and satisfies the performance criteria.

3.3. μ-Synthesis

After the entire design process done in previous sections, the robust continuous controller was obtained via μ-synthesis method [7,18] which is an iterative way of solving the mixed sensitivity problem. Three iterations were performed as there was no further progress in peak μ-value and gamma. Iteration summary is given in Table 2. Authors were unable to find a controller with better performance features. More work should be done on tuning the weighting functions in the future to receive better results.

Table 2
Iteration Summary

Iteration	1	2	3
Controller Order	4	4	6
Total D-Scale Order	0	0	2
Gamma Achieved	3690.28	120.603	98.667
Peak mu-Value	3690.28	115.393	98.664

A compensator transfer function has a structure presented in (24)

$$K(s) = \frac{b_5 s^5 + b_4 s^4 + b_3 s^3 + b_2 s^2 + b_1 s + b_0}{s^6 + a_5 s^5 + a_4 s^4 + a_3 s^3 + a_2 s^2 + a_1 s + a_0} \tag{24}$$

with the coefficients collected in Table 3:

Table 3
Robust Controller Transfer Function Coefficients

a		**b**	
a_0	1614375400828	b_0	-268719224277636
a_1	252424449491334	b_1	-42023751230480944
a_2	2687549789711	b_2	-1494702791556530
a_3	10856369937	b_3	-22344654186574
a_4	21684216	b_4	-118649007633
a_5	18400	b_5	-169446677

The obtained robust controller transfer function is of the high order and generates higher harmonic signal. In the practical application the controller (24) is converted to the discrete form with an appropriate sampling time and method. In the case of the following system, the discretisation must have been done knowingly to ensure the best control quality. Matched zeros and poles method with sampling time $T_s = 300\,\mu s$ was successfully applied in this research and the digital regulator has the z-domain structure shown in (25). Coefficients are collected in Table 4.

$$K(z) = \frac{b_5 z^5 + b_4 z^4 + b_3 z^3 + b_2 z^2 + b_1 z + b_0}{z^6 + a_5 z^5 + a_4 z^4 + a_3 z^3 + a_2 z^2 + a_1 z + a_0} \tag{25}$$

Table 4
Discrete Robust Controller Transfer Function Coefficients

a		**b**	
a_0	0.0040	b_0	7348.3765
a_1	0.7137	b_1	38363.6042
a_2	3.7700	b_2	80064.7378
a_3	8.0644	b_3	83498.2669
a_4	8.6535	b_4	43514.8709
a_5	4.6494	b_5	9066.1141

3.4. Robust Stability and Performance

Robust stability of the plant in the s-domain was checked with the theorem based on the structured singular value (μ-value) [7,18]. The experimental investigation confirmed the system stability with discrete control. The μ-value for robust stability is equal to 0.0050093 which means structured perturbations with norm less than $\frac{1}{0.0050093}$ are allowable. In other words, the stability is ensured for $\|\Delta\|_\infty < \frac{1}{0.0050093}$. The robust performance of the designed system is achieved, if and only if μ-value is less than 1 for each frequency. Unfortunately, the controller found during the research does not satisfy robust performance criteria as the maximum value of μ equals to 98.664. With respect to the robust performance it means that the size of the perturbation matrix Δ must be limited to $\|\Delta\|_\infty < \frac{1}{98.664}$.

4. Experiments

In order to ensure the same initial conditions for all objects the maximum voltage was adjusted to the electromagnet which resulted in the attachment to the coil (0 postion). The behaviour of the AMLS with the robust controller i.e. object position, object velocity and the current in a coil are depicted in Figures 5, 6 and 7, respectively.

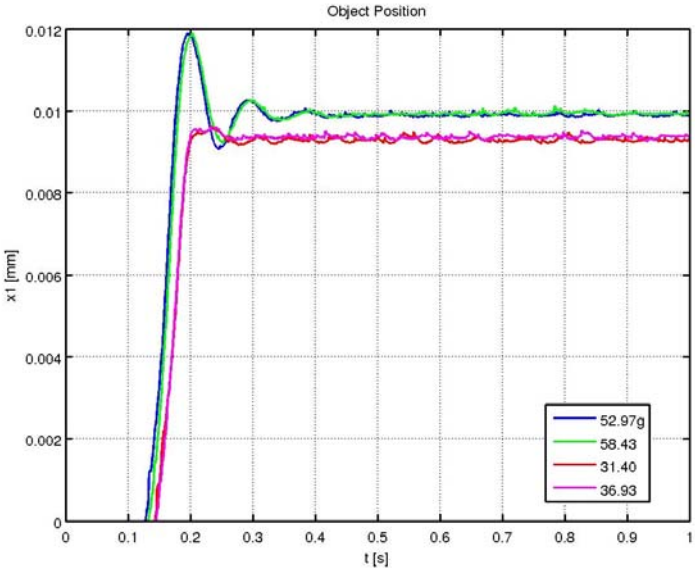

Fig. 5. Object position

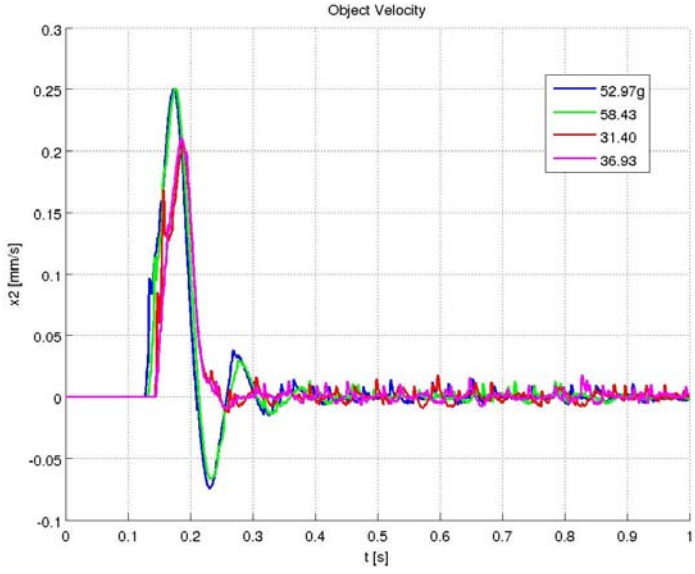

Fig. 6. Object velocity

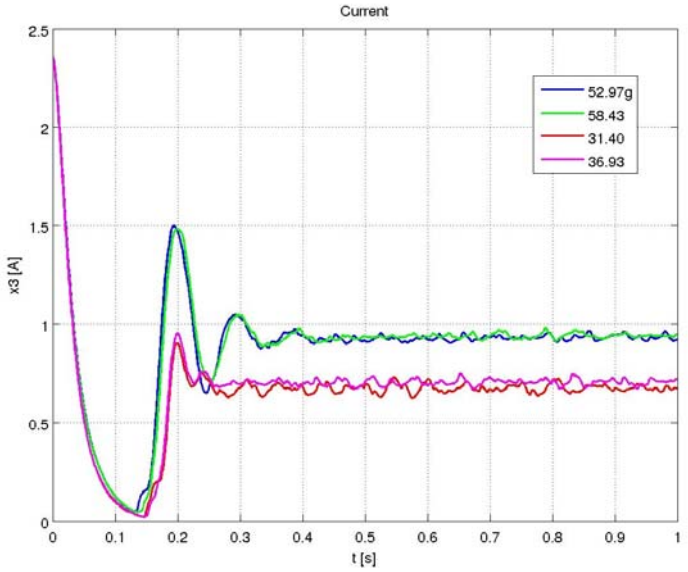

Fig. 7. Current in a coil

In contrast to 0.05297 kg and 0.05843 kg objects, objects of smaller weight were stabilised in a set position with noticeable steady-state error. On the other hand, they reached the steady state in a shorter time. Moreover, in Fig. 5 one can notice the impact of the optic sensor characteristic on the object position as objects' position change is observed at different times while current change is noticed at the same moment.

5. Conclusions

The robust compensator dedicated to the AMLS with varying mass was able to stabilise objects in the desired position with the decent performance and the steady-state error at certain level. Due to the complexity of the regulator and the presence of higher harmonics in its structure very short sampling time was necessary to make the system behave properly. In the future the weighting functions should be of higher order and be tuned maybe by genetic algorithms or other optimisation methods to achieve improvement in performance of the controller. Furthermore, information about the shape of the objects and their impact on the control task should be also included into the design process. Very interesting and promising approach may be a design of the hybrid controller combining the robust theory and e.g. fuzzy logic or neural networks. Also work on non-linear robust controller so that the compensator is invulnerable to mismatches between the model and the actual object is relevant.

References

[1] Abu-Khalaf M., Huang J., Lewis F.L. (2006). *Nonlinear H2 /H1 Constrained Feedback Control*. Springer.

[2] Alfaro-Cid E., McGookin E.W., Murray-Smith D.J. (2008). *Optimisation of the weighting functions of an H1 controller using genetic algorithms and structured genetic algorithms*. Intern. J. Syst. Sci., **39**(4), 335–347.

[3] Beaven R.W., Wright M.T., Seaward D.R. (1996). *Weighting Function Selection in the H1 Design Process*. Control Eng. Practice, **4**(5), 625–633.

[4] Bohn G. (1981). *The electromagnetic levitation and guidance technology of the 'transpid' test facility emsland*, IEEE Transactions on Magnetics, vol. MAG-20, no. 5, pp. 1666–1671.

[5] Cermák R. , Barton L., Spal P., Barták J., and Vavrík J. (2008). *Overview of Magnetic Levitation Principles and Their Application in Maglev Trains.* Advanced Engineering.

[6] Donha D.C., Katebi M.R. (2007). *Automatic weight selection for h1 controller synthesis*. Int. J. Systems Science, **38**(8), 651–664.

[7] Gu D.W., Petkov P.H., Konstantinov M.M. (2005). *Robust Control Design with MATLAB*. Springer.

[8] INTECO (2008). *Magnetic Levitation User's Guide*.

[9] Kwakernaak H. (1993). *Robust control and H1-optimization tutorial*. Pergamon Press Ltd.

[10] Mitkowski W. (1999). *Projektowanie systemów sterowania z wykorzystaniem równania riccatiego*. [in:] XIII Krajowa Konferencja Automatyki, Opole 21–24.09, vol. 1, pp. 171–176, Oficyna Wydawnicza Politechniki Opolskiej.

[11] Piłat A. (2009). *Stiffness and damping analysis for pole placement method applied to active magnetic suspension*. Automatyka: półrocznik Akademii Górniczo-Hutniczej im. Stanisława Staszica w Krakowie, **13**: 43–54.

[12] Piłat A. (2010). *μ-Synthesis of robust control to mass uncertainty in active magnetic levitation system*. 6th International Conference Mechatronic Systems and Materials, Opole, 5–8 July, 2010.

[13] Sinha P.K. (1987). *Electromagnetic Suspension – Dynamics and Control.* Peter Peregrinus.

[14] Skogesttad S., Postlethwaite I. (2000). *Multivariable Feedback Control-Anylysis and Design*. New York: John Wiley & Sons.

[15] Włodarczyk P. (2010). *Analysis and synthesis of the robust controller for a structurally unstable object*. Master's thesis, AGH University of Science and Technology, 2010. Advisor: A. Piłat.

[16] Zames G. (1981). *Feedback and optimal sensitivity: Model reference transformations, multiplicative seminorms and approximate inverses*. IEEE Transactions on Automatic Control, AC-26, 301–320.

[17] Zhou K., Doyle J., Glover K. (1996). *Robust and Optimal Control*. Prentice Hall.

[18] Zhou K., Doyle J. (1998). *Essentials of Robust Control*. Prentice Hall.